

See discussions, stats, and author profiles for this publication at: <https://www.researchgate.net/publication/262226512>

Plutonium Desorption from Mineral Surfaces at Environmental Concentrations of Hydrogen Peroxide

ARTICLE *in* ENVIRONMENTAL SCIENCE & TECHNOLOGY · MAY 2014

Impact Factor: 5.33 · DOI: 10.1021/es500984w · Source: PubMed

CITATIONS

4

READS

53

3 AUTHORS:



[James D. Begg](#)

Lawrence Livermore National Laboratory

15 PUBLICATIONS 141 CITATIONS

SEE PROFILE



[Mavrik Zavarin](#)

Lawrence Livermore National Laboratory

80 PUBLICATIONS 495 CITATIONS

SEE PROFILE



[Annie B. Kersting](#)

Lawrence Livermore National Laboratory

71 PUBLICATIONS 1,189 CITATIONS

SEE PROFILE

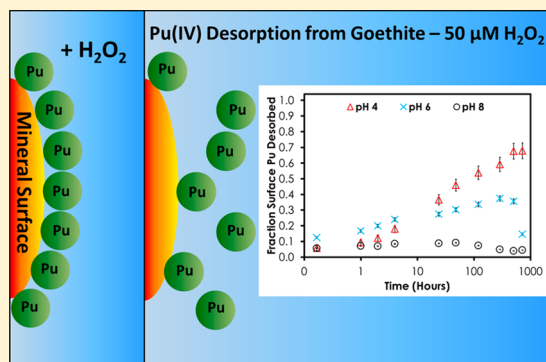
Plutonium Desorption from Mineral Surfaces at Environmental Concentrations of Hydrogen Peroxide

James D. Begg,* Mavrik Zavarin, and Annie B. Kersting

Glenn T. Seaborg Institute, Physical & Life Sciences, L-231, Lawrence Livermore National Laboratory, Livermore, California 94550, United States

S Supporting Information

ABSTRACT: Knowledge of Pu adsorption and desorption behavior on mineral surfaces is crucial for understanding its environmental mobility. Here we demonstrate that environmental concentrations of H_2O_2 can affect the stability of Pu adsorbed to goethite, montmorillonite, and quartz across a wide range of pH values. In batch experiments where Pu(IV) was adsorbed to goethite for 21 days at pH 4, 6, and 8, the addition of 5–500 μM H_2O_2 resulted in significant Pu desorption. At pH 6 and 8 this desorption was transient with readsorption of the Pu to goethite within 30 days. At pH 4, no Pu readsorption was observed. Experiments with both quartz and montmorillonite at 5 μM H_2O_2 desorbed far less Pu than in the goethite experiments highlighting the contribution of Fe redox couples in controlling Pu desorption at low H_2O_2 concentrations. Plutonium(IV) adsorbed to quartz and subsequently spiked with 500 μM H_2O_2 resulted in significant desorption of Pu, demonstrating the complexity of the desorption process. Our results provide the first evidence of H_2O_2 -driven desorption of Pu(IV) from mineral surfaces. We suggest that this reaction pathway coupled with environmental levels of hydrogen peroxide may contribute to Pu mobility in the environment.



INTRODUCTION

The production and testing of nuclear weapons, nuclear accidents, and authorized discharges of radionuclides have all contributed to a global legacy of plutonium (Pu) contamination in the environment.^{1–4} Pu contamination in the environment is a topic of key concern because of its radiological toxicity and long half-life (24 100 years for ^{239}Pu). A wide array of factors can significantly influence Pu mobility in natural systems including redox processes,^{5,6} colloid-facilitated transport processes,^{7–9} solubility effects,^{10,11} sorption/desorption rates and affinities for natural mineral surfaces,^{12–14} and interactions with natural organic matter (including bacteria).^{15,16} One of the outstanding issues currently limiting the development of reliable predictive transport models involves understanding the rates and mechanisms of Pu sorption to, and desorption from, mineral surfaces in the presence of water.

Under environmental conditions Pu can exist in multiple oxidation states (Pu(VI), Pu(V), Pu(IV), and Pu(III)) with each oxidation state displaying a unique solubility¹⁰ and sorption affinity.^{12,17–19} Importantly, redox kinetics can be rate limited, which may lead to transient, nonequilibrium oxidation states.^{12,14} Pu(VI) may occur in highly oxic waters, such as rainwaters, but it is expected to rapidly reduce to Pu(V) in most other natural waters.^{20,21} In oxic environments, such as in surface waters, Pu in the aqueous phase is predominantly expected to occur in the pentavalent state.^{5,20,21} Due to effective charge considerations, Pu(V) is also expected to be the most mobile oxidation state of Pu, displaying a low adsorption

affinity for mineral surfaces. In the presence of organic and inorganic material (including mineral surfaces), Pu(V) has been shown to reduce to Pu(IV).^{18,22–25} For example, the adsorption of Pu(V) to the iron oxyhydroxide mineral goethite (αFeOOH) is thought to result in the reduction of Pu(V) to Pu(IV) on the mineral surface, driving further adsorption of aqueous Pu(V).^{18,23} Similar surface-mediated redox processes have been observed on montmorillonite and quartz surfaces.^{12,26,27} In suboxic subsurface waters, Pu is predominantly expected to occur in the tetravalent state, which has been shown to have a far greater adsorption affinity for mineral surfaces than either Pu(III), Pu(V), or Pu(VI).^{5,18,21,25,28,29} Therefore, the Pu(IV) oxidation state is likely to be the most important oxidation state of Pu associated with mineral surfaces. Pu(III) has only been detected under simulated anoxic environmental conditions.^{28,30,31}

The desorption of Pu from mineral surfaces has received less attention than adsorption although it will also ultimately play a key role in determining the extent of aqueous Pu environmental transport. Typically, batch desorption experiments demonstrate that Pu largely remains associated with the mineral surface. For example, Pu batch desorption experiments with goethite and hematite have indicated that less than 1% of the Pu associated

Received: February 26, 2014

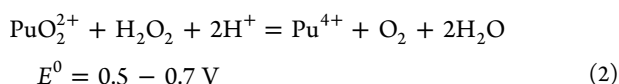
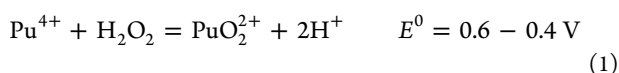
Revised: May 2, 2014

Accepted: May 9, 2014

with the mineral surface will be desorbed.³² Similarly, experiments with sediments from the Esk Estuary, UK showed that about 5% of Pu associated with the sediments (which was predominantly in the Pu(III)/(IV) oxidation state on the sediment surface) could be desorbed.³³ Similar values were measured for Pu desorbed from Aiken, SC sediments³⁴ where approximately 1–9% of adsorbed Pu was removed in batch experiments across a pH range from 2.4 to 8.4. Greater extents of Pu desorption have been reported for montmorillonite and silica, where up to 20% of Pu was desorbed after ~300 days in batch experiments at pH ~8.¹⁴

The oxidation state of Pu is also important in controlling both the rate and extent of Pu desorption from mineral surfaces.^{14,32–34} For example, the Pu, which was initially present on the solid surface as Pu(IV), in the Aiken, SC sediments was found to be present in solution as Pu(V) following a desorption period of 33 days.³⁴ In this case it was proposed that the oxidation of Pu(IV) to Pu(V) on the mineral surface was the mechanism behind the Pu(IV) desorption. Further, the desorption of Pu(IV) from Irish Sea sediments was found to increase when they were exposed to natural sunlight.³⁵ The sunlight was thought to cause the photooxidation of surface Pu(IV) to Pu(V) which was subsequently more readily desorbed. This redox-driven remobilization is consistent with the behavior of other redox active radionuclides, such as Tc, Np, and U, where oxidation of reduced, solid-associated species results in their remobilization.^{36–40}

High concentrations of H₂O₂ (~0.01–0.1 M) are known to alter the oxidation state of Pu^{6,41} and are used in the purification and separation of waste streams as well as the preparation of Pu stock solutions for use in experimental work (e.g., Clark et al., 2011).⁴² Hydrogen peroxide can be used to reduce Pu(V) or Pu(VI) to Pu(IV) and to precipitate Pu(IV) from acidic solution.^{41,43} Oxidation of Pu(OH)₄ by H₂O₂ in 4 M NaOH solution has also been demonstrated.⁴⁴ These results are consistent with half-cell reactions which demonstrate that both oxidation and reduction of Pu by hydrogen peroxide is possible (eqs 1 and 2).⁴⁵

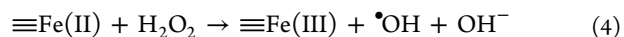
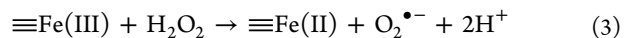


It has been suggested that in seawater and at concentrations as low as 1×10^{-5} M, H₂O₂ may enhance the reduction of Pu(V) to Pu(IV), thus potentially decreasing the mobility of Pu(V) species.⁶

Hydrogen peroxide is present in natural water bodies as a result of various processes including photochemical reactions mediated by natural organic matter, input from rainwater, and metabolic processes of fungi and bacteria.^{46–49} Concentrations up to 40 μM have been measured in rainwater while in soils, H₂O₂ generated by fungi and bacteria can result in concentrations between 2 and 15 μM in the surrounding microenvironment.^{46,48–51} Indeed, it has recently been proposed that H₂O₂ produced by subsurface bacteria may enhance the oxidation of contaminant iodide species with associated implications for the environmental mobility of ¹²⁹I.⁵² Finally, in nuclear waste repository scenarios, groundwater adjacent to spent nuclear fuel will be exposed to ionizing

radiation resulting in the production of H₂O₂ at concentrations of 1–1000 μM.^{53–55}

It has been demonstrated that the decomposition of H₂O₂ is catalyzed in the presence of Fe(II)/(III) species resulting in the production of reactive oxygen species (ROS) such as O₂^{•−} and OH[•].^{56–59} The generation of these ROS is pH dependent and is an area of active research. Illustrative reactions are shown in eqs 3 and 4.



The ROS can enhance oxidation of organic matter or metals and may be more effective oxidizers than H₂O₂ alone.^{56–58,60} This oxidation can also extend to species, such as As(III), adsorbed to the surface of iron(hydr)oxide minerals, and may exert an important control on their environmental mobility.^{58,59} Further, recent work has demonstrated that alpha radiolysis induced by ²³⁸Pu can, in the presence of Fe(II), lead to the production of a sufficient concentration of H₂O₂ to cause the oxidative dissolution of PuO₂.⁵⁵ To our knowledge, there have been no studies examining the effect of H₂O₂ on Pu adsorbed to the surface of common minerals at environmentally relevant H₂O₂ concentrations.

Here we demonstrate that the desorption of Pu(IV) adsorbed onto mineral surfaces is caused by the presence of environmental concentrations of H₂O₂. In our study, Pu(IV) was adsorbed to the surface of goethite (αFeOOH), montmorillonite (2:1 dioctahedral clay), and high purity quartz (SiO₂) for a minimum of 21 days. H₂O₂ was then spiked into Pu-mineral suspensions and the aqueous Pu concentration monitored. H₂O₂ concentrations in the experiments ranged from 5 to 500 μM and are broadly comparable to measured rainwater values (<2 μM to 40 μM), concentrations generated by some bacteria (2–15 μM) and concentrations likely to exist in nuclear repository environments as a result of radiolysis reactions (1–1000 μM).^{46,48–51}

MATERIALS AND METHODS

Plutonium Stock Preparation. A ²³⁸Pu stock (99.8% ²³⁸Pu, 0.1% ²⁴¹Pu, and 0.1% ²³⁹Pu by activity) was used in all experiments. The Pu stock solution was purified using an anion exchange resin (BioRad AG 1 × 8, 100–200 mesh) preconditioned with 8 M HNO₃. Prior to loading on the resin, Pu was reacted with NaNO₂ to reduce it to Pu(IV). The Pu was loaded on the resin in 8 M HNO₃, washed with three column volumes of 8 M HNO₃, and then eluted in 0.1 M HCl.⁶¹ The oxidation state of the Pu stock was checked with a LaF₃ precipitation method⁶² and found to be >99% Pu(III)/(IV).

Mineral Preparation. All solutions were prepared using ultrapure water (Milli-Q Gradient System, >18 MΩ·cm) and ACS grade chemicals without further purification. The SWy-1 montmorillonite (Source Clays Repository of the Clay Minerals Society) was treated with 0.001 M HCl and 0.03 M H₂O₂ to remove organic matter and free iron oxides, Na-homoionized, and washed thoroughly in MQ water. Details regarding this and the preparation of goethite were reported previously.^{12,26,61,63} The Iota 8 high purity quartz was obtained from Unimin Corporation (Spruce Pine, NC) and was ground in a ball mill to increase surface area; no other pretreatment was performed. Surface areas were $20.6 \pm 0.6 \text{ m}^2 \text{ g}^{-1}$ for goethite, $31.5 \pm 0.2 \text{ m}^2 \text{ g}^{-1}$ for montmorillonite, and $2.1 \pm 0.2 \text{ m}^2 \text{ g}^{-1}$ for quartz

($N_2(g)$ -BET, Quadrasorb SI). The amount of extractable Fe in the montmorillonite removed by 0.5 N HCl was 530 ppm.^{12,64} The Fe content of Iota 8 high purity quartz is reported to be <0.05 ppm (Unimin Corporation, Spruce Pine, NC).⁶⁵

Hydrogen Peroxide Desorption Experiments. Minerals were initially suspended in a 0.7 mM $NaHCO_3$, 5 mM NaCl buffer solution. Goethite suspensions were prepared with a solid–solution concentration of 0.1 g L^{-1} , and montmorillonite and quartz suspensions had a concentration of 1 g L^{-1} . Suspensions were spiked with Pu(IV) to a final concentration of 3×10^{-10} M which is expected to be below the solubility of Pu(IV). Dilute HCl and NaOH were then used to adjust the pH of the mineral suspensions to 4, 6, and 8 ± 0.2 units. The suspensions were allowed to equilibrate in the dark at room temperature for 21 days to establish a steady state in the experiments prior to H_2O_2 addition and the pH monitored periodically and adjusted as needed. Typical drift was less than 0.3 units during this period. Total volumes of HCl and NaOH added comprised less than 0.5% of the total suspension volume in all cases.

Following this equilibration period, aliquots of the suspension were removed and centrifuged at 10 000g for 30 min to achieve a particle size cutoff of 60 nm. The Pu concentration in the supernatant was determined by liquid scintillation counting (LSC; Packard Tri-Carb TR2900 LSA and Ultima Gold cocktail). Aliquots (35 mL) of the original suspensions were transferred to clean Nalgene Oak Ridge polycarbonate centrifuge tubes and spiked with a H_2O_2 stock prepared by dilution of a 30% H_2O_2 solution with Milli-Q water just before use. The concentration of the H_2O_2 stock was verified by measuring its absorbance at 240 nm.⁶⁶ Final H_2O_2 concentrations were 5, 50, and 500 μM in goethite experiments, 5 and 500 μM in quartz experiments, and 5 μM in montmorillonite experiments. The tubes were wrapped in aluminum foil to minimize photochemical reactions and placed on an orbital shaker at 125 rpm at room temperature.

To measure desorption of Pu from mineral surfaces, aliquots of the suspensions were withdrawn and centrifuged, and the Pu concentration in the supernatant was determined by LSC. Pu desorption was typically monitored over a 30 day (720 h) period. Supernatant Fe_{total} concentration in goethite experiments at early time points was measured using the Ferrozine method described by Viollier et al.⁶⁷ The pH of the 5 and 50 μM H_2O_2 goethite experiments, the 5 μM H_2O_2 montmorillonite experiment, and the 500 μM H_2O_2 quartz experiment was measured after 21 days and was typically found to have drifted by less than 0.2 units from pre- H_2O_2 values.

Three terms are used to describe the sorption/desorption behavior of Pu in the current work. The first of these is K_d (mL g^{-1}), which was calculated after the 21 day adsorption period from the measured bulk Pu suspension concentration (C_{Bulk} , M), supernatant Pu concentration (C_0 , M), and the mineral suspension concentration ([mineral], g mL^{-1}) as follows:

$$K_d = \frac{C_{Bulk} - C_0}{C_0} \frac{1}{[\text{mineral}]} \quad (5)$$

Typically, K_d values are used to imply an equilibrium distribution coefficient. However, in these experiments equilibrium was most likely not achieved because of the complexity of Pu oxidation state transformations on both mineral surfaces and in solution. As a result, we consider K_d in

this work to be a conditional K_d used simply to characterize the distribution of Pu between the solid and the aqueous phase.

The second term is “desorbed Pu” (C_{des} , M), which refers to the concentration of Pu desorbed from the mineral surface and is calculated by subtracting the aqueous Pu concentration at the time suspensions were spiked with H_2O_2 from the concentration of Pu at each time point. C_{des} was calculated as

$$C_{des} = C - C_0 \quad (6)$$

where C (M) is the concentration of Pu in solution at the sampling time point and C_0 (M) the concentration of Pu in the supernatant after the 21 day adsorption equilibration period. C_{des} allows comparison of the absolute concentration of Pu desorbed from the mineral surface in these experiments because the initial amount of Pu adsorbed to the mineral surface varies as a function of pH and mineral type. Because of the way C_{des} is calculated, it is possible to obtain negative values for this term as readsorption processes can result in Pu solution concentrations falling below values measured at the start of the H_2O_2 experiments.

Finally, C_{des} is also expressed as a percentage of the initial Pu concentration on the mineral surface such that

$$\text{percent surface Pu desorbed} = \frac{C_{des}}{C_{Bulk} - C_0} \times 100\% \quad (7)$$

To characterize H_2O_2 decomposition in the presence of goethite, a set of Pu-free goethite experiments was performed at pH 4, 6, and 8 with 50 μM H_2O_2 . The H_2O_2 concentration in the supernatant was measured as a function of time using Amplex Red reagent (Life Technologies, CA).⁶⁸ Standard calibrations were run at each sampling point and returned R^2 values of 0.99 or better (detection limit is 0.1 μM).⁶⁹

Flow Cell Experiment. To complement the batch experiments, a stirred flow cell experiment was performed with goethite at pH 8. The flow cell set up was similar to that described previously for Np(V) reaction with goethite.⁶³ The flow cell was made of Teflon with a 20 mL hemispherical chamber. A diagram of the flow cell is shown in Supporting Information (SI) Figure S1. Prior to use, the cell was washed with 10% HCl and MQ water. A 20 mL aliquot of the 21 day Pu-goethite equilibrated suspension at pH 8 (0.1 g L^{-1}) was placed in the flow cell along with a stir bar and 0.7 mM $NaHCO_3$, 5 mM NaCl buffer solution at pH 8 was then pumped through the cell at a rate of 0.4 mL min^{-1} (retention time of 50 min) for three chamber volumes. After this period, the influent solution was changed to a buffer solution spiked with 10 μM H_2O_2 at a rate of 0.4 mL min^{-1} for seven chamber volumes. Effluent fractions were collected on a Spectra/Chrom CF-1 fraction collector and the volumes determined gravimetrically. Pu concentration was determined via LSC as described previously.

RESULTS AND DISCUSSION

Adsorption of Pu(IV) to Goethite, Montmorillonite, and Quartz. The adsorption of Pu(IV) to all minerals following the 21 day adsorption equilibration period is reported in terms of $\log K_d$ in Table 1. Previous experiments in our laboratory examining Pu(IV) adsorption to goethite, montmorillonite, and quartz suggest that a conservative K_d error of 15% is applicable to these values. The K_d data show that the adsorption of Pu(IV) is strongly affected by both pH and mineral type. Furthermore, the pH-dependence is unique to

Table 1. Calculated $\log K_d$ (mL g^{-1}) Pu(IV) Values for Goethite, Montmorillonite, and Quartz as a Function of pH Value Following 21 Days Equilibrium in 0.7 mM NaHCO_3 , 5 mM NaCl Buffer Solution^a

mineral	pH 4	pH 6	pH 8
goethite	4.4	5.3	6.2
montmorillonite	6.3	4.9	4.5
quartz	3.2	4.0	3.7

^aResults are from one replicate. The estimated error in these $\log K_d$ values is ± 0.1 based on previous work in our laboratory (see text).

each mineral. In the case of goethite, the extent of adsorption was lowest at pH 4 and highest at pH 8. For montmorillonite, the highest Pu(IV) adsorption is at pH 4 after which adsorption decreases with increasing pH. Pu(IV) sorption to quartz was

lower than for montmorillonite and goethite and shows a maximum K_d value at pH 6. The K_d values obtained in the current work for goethite and quartz are broadly consistent with those calculated from previous adsorption studies for goethite¹⁸ and quartz.²⁷ For montmorillonite, which to our knowledge has been the subject of fewer Pu adsorption studies, the $\log K_d$ value at pH 8 of 4.5 is similar to the value of 4.3 obtained previously in a comparable isotherm experiment with 10^{-10} M Pu(IV).¹²

Pu(IV)–Goethite– H_2O_2 Interactions. Addition of H_2O_2 to systems containing Pu(IV) adsorbed to goethite resulted in the desorption of Pu(IV) from the goethite surface (Figure 1). The extent of desorption showed a pH dependency such that the amount of Pu desorbed at pH 4 > pH 6 >> pH 8. At pH 4, the Pu continues to be removed from the goethite surface throughout the experiment (720 h). In contrast, at pH 6 and 8,

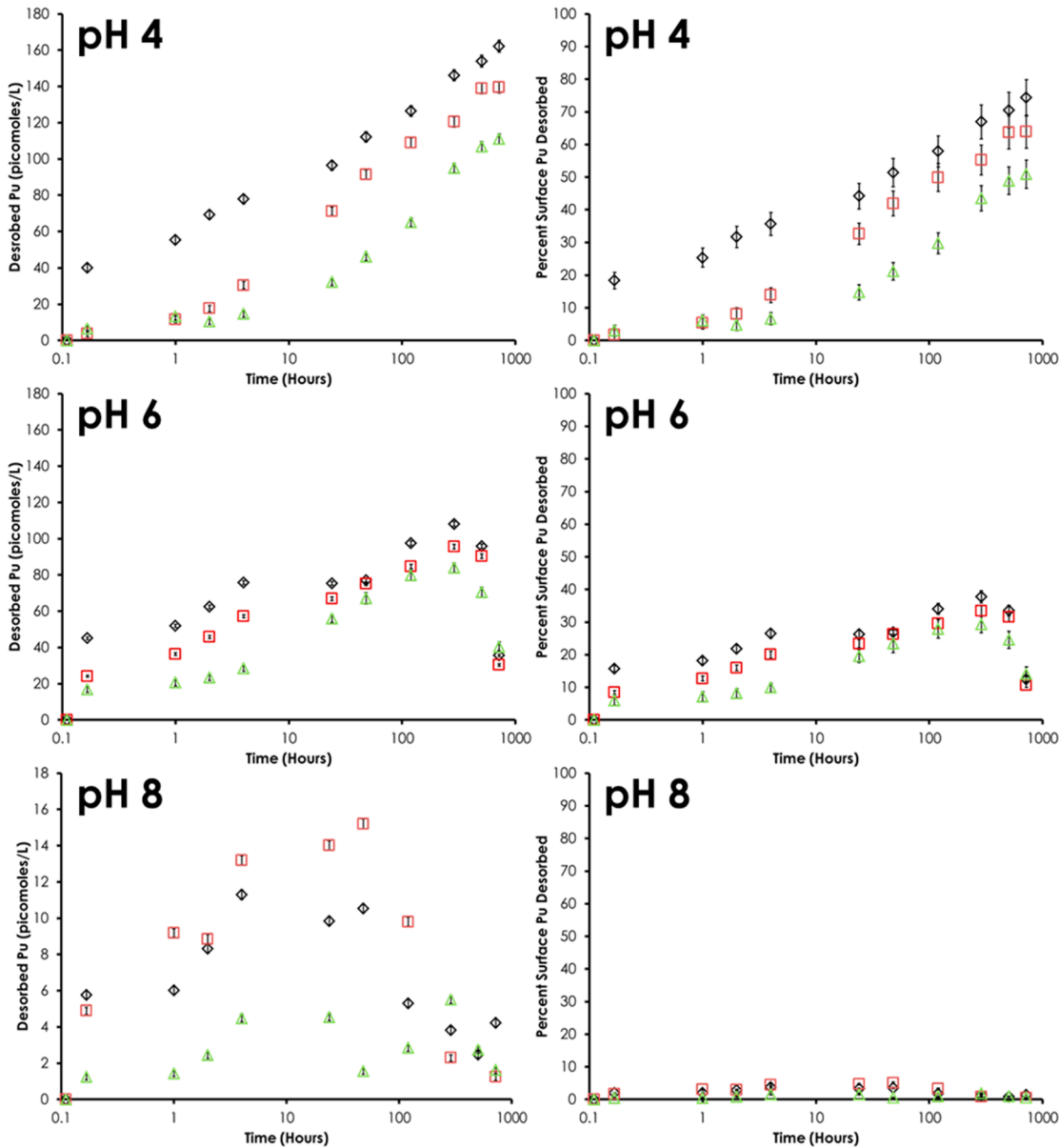


Figure 1. Pu desorption from goethite with time (C_{des}) following addition of the following: 5×10^{-4} M H_2O_2 (diamonds); 5×10^{-5} M H_2O_2 (squares); 5×10^{-6} M H_2O_2 (triangles). Experiments performed in 0.7 mM NaHCO_3 , 5 mM NaCl buffer solution with 0.1 g L^{-1} goethite. Left side plots show calculated desorbed Pu concentrations; right side plots show desorbed Pu plotted as a percentage of initial surface Pu concentrations (see text for details). Error bars based on propagation of 2s % LSC uncertainties. Please note difference in y-axis scale in left side pH 8 plot.

desorption had stopped and readsorption of Pu from solution had started to occur by the end of the experiment as evidenced by a decline in desorbed Pu concentration.

In batch experiments, the maximum desorption of Pu was observed at pH 4 with a H_2O_2 concentration of 500 μM where 74% of the Pu initially associated with the goethite was desorbed. The lowest maximum desorption observed was at pH 8 with a H_2O_2 concentration of 5 μM in which 1.8% of the surface Pu was desorbed after 288 h. This value is significantly larger than the <1% desorption of Pu from goethite at pH 8.25 reported by Lu et al.³² Importantly, for experiments at circumneutral pH values, significant desorption of surface Pu was observed at environmentally relevant concentrations of 5 μM (pH 6, 29.3%; pH 8, 1.8%) and 50 μM (pH 6, 33.4%; pH 8, 5.1%) H_2O_2 .^{48–50} Thus, our results suggest that the desorption of Pu(IV) adsorbed to goethite surfaces in natural environments could be promoted by the presence of H_2O_2 .

Apparent rates of Pu desorption from goethite in the first 4 h of the experiment were calculated and are plotted as a function of H_2O_2 concentration in SI Figure S2. For experiments at pH 4 and 6, the early time rates of Pu desorption are similar. In all experiments, the rates are substantially greater at 50 and 500 μM H_2O_2 than at 5 μM . However, a simple first-order dependence on H_2O_2 concentration is not observed. This suggests that H_2O_2 may not be the rate-limiting species for desorption but that it may be a product of H_2O_2 decomposition which controls Pu desorption. At pH 8, apparent desorption rates are much lower than at pH 4 and pH 6 for all H_2O_2 concentrations. The desorption rate at pH 8 with a H_2O_2 concentration of 5 μM is again lower than the rate at 50 μM and 500 μM , but the difference is much less marked than for experiments at pH 4 and 6.

To examine the relationship between H_2O_2 decomposition and Pu desorption, H_2O_2 concentrations were measured in Pu-free goethite experiments spiked with 50 μM H_2O_2 . Figure 2 shows that a decline in H_2O_2 concentration occurs over time at all pH values. After 192 h, over 94% of H_2O_2 had been lost from solution in all experiments. Pseudo-first-order rate constants were calculated for the first 96 h of H_2O_2 loss from

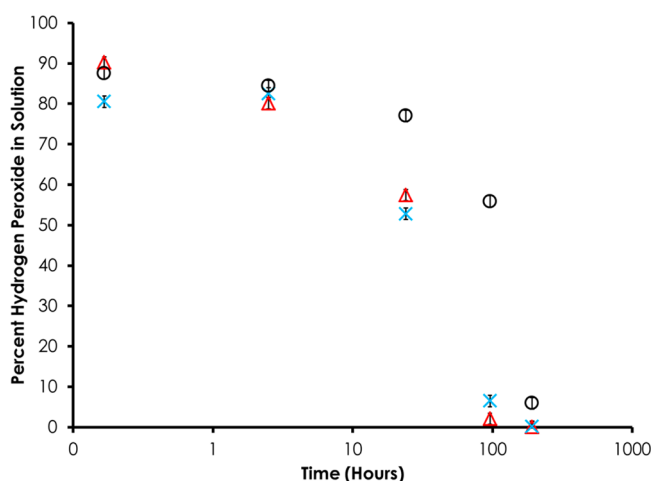


Figure 2. H_2O_2 loss from solution in parallel, Pu-free, 0.1 g L^{-1} goethite/0.7 mM NaHCO_3 , 5 mM NaCl buffer suspensions. Experiments performed at initial pH values of 4 (triangles), 6 (crosses), and 8 (circles) and spiked with 5×10^{-5} M H_2O_2 . Errors extrapolated from the standard deviation of triplicate sample measurement at 192 h.

solution. Data were surface area normalized to facilitate comparison with other work. Rates were 0.019 $\text{h}^{-1} \text{m}^{-2}$, 0.013 $\text{h}^{-1} \text{m}^{-2}$, and 0.002 $\text{h}^{-1} \text{m}^{-2}$ at pH 4, 6 and 8, respectively. A pH dependency on the rate of H_2O_2 decomposition in the presence of an iron oxyhydroxide mineral has been observed previously.^{59,70,71} Our rates of H_2O_2 decomposition are comparable to previously published surface area normalized H_2O_2 decomposition rates in the presence of goethite at pH ~ 7 of 0.0098 $\text{h}^{-1} \text{m}^{-2}$ and 0.0012 $\text{h}^{-1} \text{m}^{-2}$.⁷¹

Comparison of these parallel Pu-free experiments (Figure 2) with Pu-containing experiments at 50 μM H_2O_2 (Figure 1) indicates that the apparent rate/extent of Pu desorption is broadly proportional to the rate of H_2O_2 loss. For example, H_2O_2 decomposition rates at pH 4 and pH 6 are comparable to each other and are significantly greater than the rate at pH 8. Similarly, initial Pu desorption rates at pH 4 and 6 are alike and greater than the rate at pH 8. It is important to note that while the parallel Pu-free experiment at pH 4 shows that H_2O_2 has been largely removed from solution after 100 h of reaction time (Figure 2), in the equivalent Pu-containing experiment, Pu continues to be desorbed from the goethite surface (Figure 1). In contrast, at pH 8, the Pu concentration in solution begins to fall after 48 h despite the parallel H_2O_2 experiment indicating that there will still be significant H_2O_2 remaining in solution at this time (Figure 1; Figure 2). This suggests that it is H_2O_2 decomposition products and not H_2O_2 that drive Pu desorption. Further work is needed to elucidate the species responsible for promoting Pu desorption at different pH values.

Mechanisms for Pu Desorption. To test whether goethite dissolution was responsible for Pu desorption from goethite, the concentration of Fe in solution was measured at early time points. However, no significant Fe was detected in solution during the first 48 h of the experiment via spectrophotometric analysis (estimated detection limit 0.3 μM). Further, measurement of all the supernatants by ICP-MS after 12 days of reaction showed that Fe concentrations were below 2 μM and did not differ significantly from pre H_2O_2 spike concentrations (data not shown). This indicates that the observed desorption of Pu is not the result of goethite dissolution.

It is likely that changes in Pu oxidation state will contribute to the desorption of Pu(IV) in these experiments given that Pu(III), Pu(V), and Pu(VI) species all have a lower sorption affinity for goethite than Pu(IV).^{18,25,29} Because of the low Pu concentrations used in this study, the complex nature of aqueous Pu oxidation state distribution, and the relatively fast time scales of the Pu desorption observed here, traditional indirect methods of assessing Pu oxidation state in solution (e.g., LaF_3 precipitation, solvent extraction) were unable to definitively characterize these systems. However, the results of aqueous Pu oxidation state measurements in experiments at pH 4 and pH 6 at 500 μM H_2O_2 , where the most Pu desorption is observed, show that the predominant aqueous oxidation state changes from Pu(III)/(IV) to Pu(V)/(VI) over the course of the experiment. In parallel mineral-free and H_2O_2 -free experiments, this oxidation state change was not observed. A more detailed discussion of these data is included in the SI. Previously, Fenton-type reactions between H_2O_2 and Fe(III) have been shown to produce ROS capable of altering the oxidation state of As(III) adsorbed to a ferrihydrite, leading to potential changes in its sorption behavior.⁵⁹ Thus, it is likely that H_2O_2 interaction with Fe(III) results in the production of ROS which act to alter the oxidation state of sorbed Pu(IV),

most likely to Pu(V) or Pu(VI), leading to its desorption from the mineral surface.

Readsorption of Pu by Goethite. As mentioned previously, a noticeable aspect of the pH 6 and pH 8 desorption plots in Figure 1 is that at all H_2O_2 concentrations investigated, a percentage of the Pu which was initially desorbed is subsequently readsorbed on the goethite surface. The readsorption was not observed at pH 4 over the time scale of these experiments (30 days). The initial desorption followed by readsorption of Pu suggests that there are at least two competing processes with different kinetic rates occurring in these systems: a “forward” H_2O_2 -driven Pu desorption process and a “reverse” Pu readsorption process. Thus, the apparent extent of desorption at any one time in these experiments is both a function of the “forward” H_2O_2 -driven desorption (H_2O_2 -driven Pu(IV) oxidation and desorption) and also of the rate of the “reverse” readsorption/surface-mediated reduction. The faster readsorption/surface-mediated reduction observed here with increasing pH is consistent with the pH-dependent surface-mediated Pu(V) reduction rates on goethite reported by Powell et al.²³

Pu adsorption to goethite exhibits a pH dependency in these experiments and is greatest at pH 8 (Table 1). Additionally, the reaction of H_2O_2 with Fe(III) and the nature of the ROS formed has been shown to be pH dependent.⁵⁹ Thus, we propose that the lower level of desorption observed at pH 8 is a function of both the limited efficacy of the forward H_2O_2 -driven desorption and the strong adsorption affinity of Pu for goethite at this pH. Further, the readsorption, which is also seen at pH 6, likely results from a loss of effective ROS species in the batch system and hence a loss of driver for the forward desorption reaction. In contrast, at pH 4, the forward reaction is not only more effective but the adsorption affinity of Pu (especially Pu(V)) for goethite is much lower than at pH 8.²³ This interplay of forward and reverse processes is likely to have implications for the H_2O_2 influenced mobility of Pu in natural environments.

Goethite Flow Cell Experiment. The flow cell experiment was performed with 10 μM H_2O_2 to confirm that the readsorption of Pu observed in the batch goethite experiments at pH 8 was caused by a decline in H_2O_2 /ROS concentration. Figure 3 shows the cumulative fraction of surface Pu desorbed from the goethite during the flow cell experiment. Minimal Pu was desorbed from the goethite when the influent solution was the 0.7 mM NaHCO_3 , 5 mM NaCl buffer solution at pH 8. However, when the influent solution was spiked with H_2O_2 (indicated by the dashed red line in Figure 3), a significantly higher concentration of Pu was desorbed. Continuous desorption of Pu from the goethite was observed for the duration of the flow cell experiment. At the termination of the experiment, the amount of surface Pu desorbed was 3.2% compared to batch experiments at pH 8 with 5 and 50 μM H_2O_2 where maximum surface desorption was 1.8% and 5.1%, respectively. The continuous removal of Pu from the goethite surface as opposed to the readsorption in the batch experiments also demonstrates that it is a decline in the efficiency of the “forward” H_2O_2 -driven desorption which leads to the readsorption of Pu seen in batch experiments at pH 8. However, it must also be pointed out that Pu removed in the flow-cell effluent cannot physically be readsorbed. From an environmental standpoint, this suggests that the continued presence of H_2O_2 in the environment will lead to significant desorption of Pu from the surface of iron-containing minerals at circum-

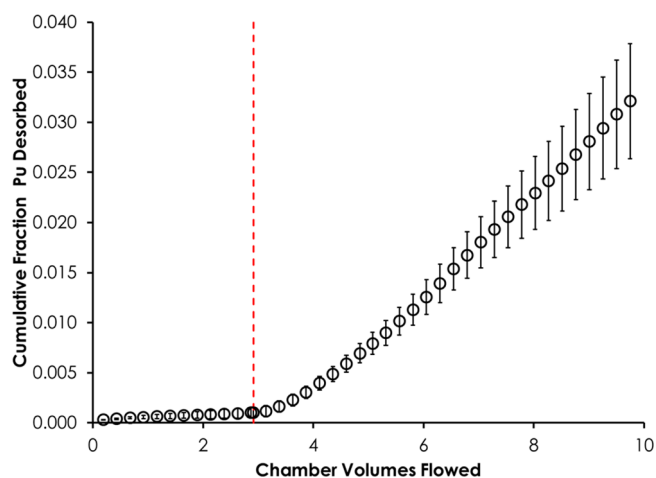


Figure 3. Experimental results from Pu(IV)–goethite desorption flow-cell experiment performed with 3×10^{-10} M Pu_{Bulk} and 0.1 g L^{-1} goethite at pH 8. Initially the influent solution was Pu-free 0.7 mM NaHCO_3 , 5 mM NaCl buffer at pH 8. After three chamber volumes, the buffer was spiked with 1×10^{-5} M H_2O_2 (denoted by dashed red line). Influent flow rate was 0.4 mL min^{-1} (50 min average retention time). Error bars based on propagation of LSC uncertainties.

neutral pH. In contrast, transient production of H_2O_2 by natural processes would result in a temporary desorption of Pu.

Pu(IV)–Quartz– H_2O_2 and Pu(IV)–Montmorillonite– H_2O_2 Interactions. Plutonium– H_2O_2 desorption experiments were also performed with quartz and montmorillonite at a H_2O_2 concentration of 5 μM . These experiments were carried out to determine if environmental concentrations of H_2O_2 could drive desorption of Pu from a mineral surface lacking an obvious catalytic iron species. Figure 4 shows that H_2O_2 -driven desorption of Pu from the quartz and montmorillonite surfaces occurs to some degree and in a transient manner at all three pH values. However, the extent of desorption is much less pronounced than that observed in the corresponding goethite experiments. We note the increased scatter in the data in the quartz experiments which we attribute in part to the lower initial adsorption of Pu(IV) onto quartz. The desorption of Pu from both quartz and montmorillonite was transitory at all pH values with Pu concentrations declining to values at least equal to or less than initial solution concentrations by the end of the experiment, leading to negative desorbed Pu concentrations in Figure 4.

Although these results suggest that the presence of H_2O_2 at environmental concentrations can promote desorption of Pu from quartz and montmorillonite, it also highlights the importance of reactive Fe in the desorption process at low H_2O_2 concentrations. Future work is planned to investigate whether ROS formed by the decomposition of H_2O_2 in the presence of goethite can enhance the desorption of Pu from adjacent mineral surfaces such as montmorillonite and quartz.

A final experiment was performed with quartz and H_2O_2 at 500 μM H_2O_2 . SI Figure S4 shows that Pu desorption was much more pronounced at this higher H_2O_2 concentration. The extent of Pu desorption is surprising given that there is no obvious source of catalyst for the Fenton-type heterogeneous oxidation which is posited to drive Pu desorption from goethite. Measurement of Si in solution after 12 days of reaction indicated that some dissolution of quartz occurred in these experiments following addition of H_2O_2 (data not shown) so we cannot rule out a dissolution-driven desorption process in

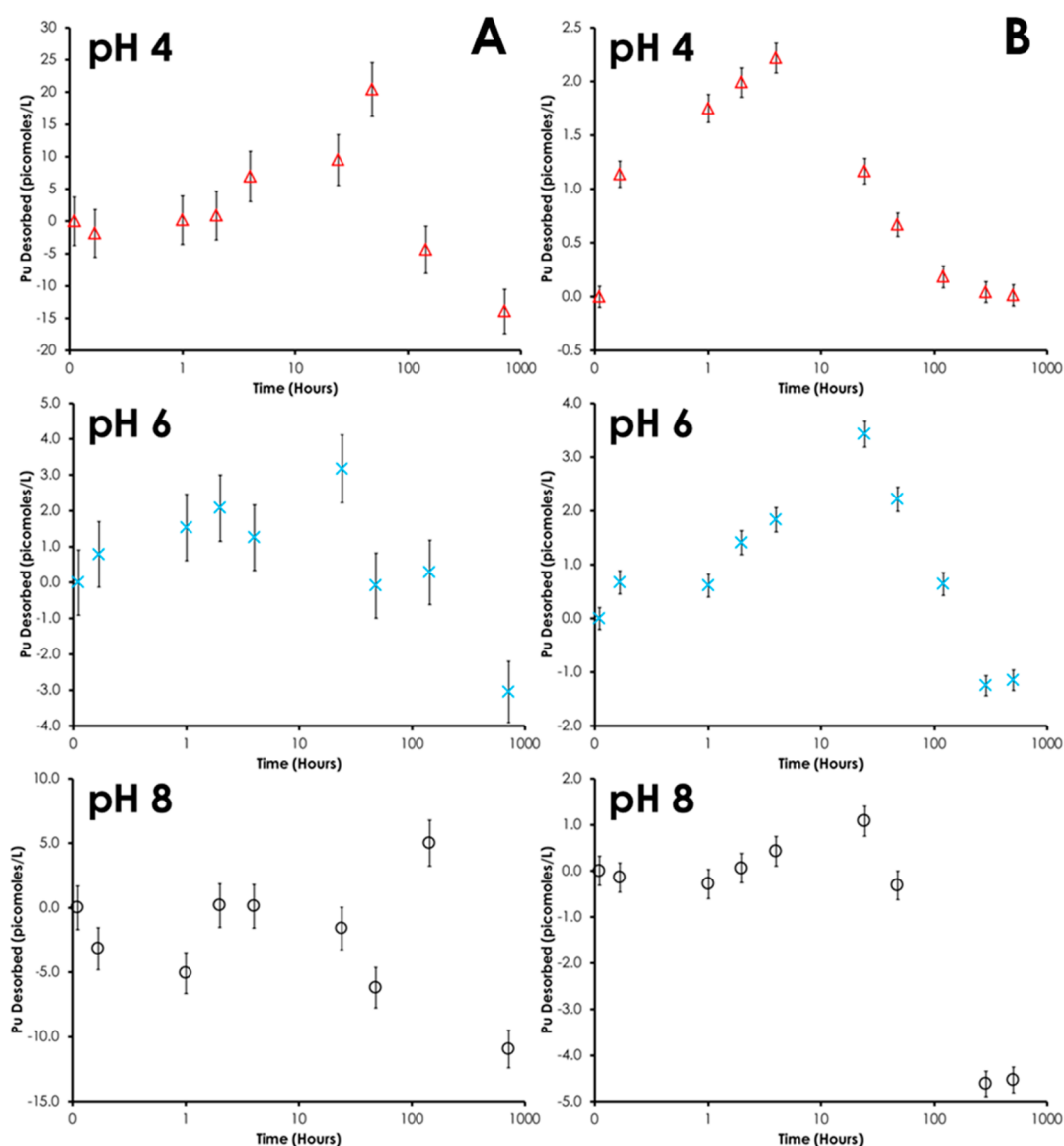


Figure 4. Desorption of Pu (C_{des}) from (A) quartz and (B) montmorillonite following addition of 5×10^{-6} M H_2O_2 . Experiments performed in 0.7 mM $NaHCO_3$, 5 mM $NaCl$ buffer solution with 1 g L^{-1} mineral. Note the difference in y-axis scale between the two minerals and the different pH values. Values may be negative if Pu concentrations fall below the concentration at the start of the experiment. Error bars based on propagation of 2% LSC uncertainties.

these experiments. Nonetheless, the data indicate that given sufficient H_2O_2 concentration, Pu(IV) can be desorbed from a silicate mineral in the absence of Fe. However, we also note that $500 \mu\text{M}$ H_2O_2 is at least 1 order of magnitude greater than environmental H_2O_2 concentrations. The difference in Pu desorption behavior between quartz at $500 \mu\text{M}$ and $5 \mu\text{M}$ highlights both the complexity of mineral–contaminant– H_2O_2 reactions and the importance of using environmentally relevant H_2O_2 concentrations when investigating environmental, H_2O_2 -driven reactions.

ENVIRONMENTAL IMPLICATIONS

Previously, it was suggested by Morgenstern and Choppin that the presence of H_2O_2 in the environment may enhance the rate of Pu(V) reduction in natural waters, potentially limiting its environmental mobility.⁶ In the current study, we show that Pu(IV) adsorbed to the surface of goethite experiences a pH-dependent desorption in the presence of environmentally

relevant concentrations of H_2O_2 . The presence of environmental concentrations of H_2O_2 also caused desorption of Pu from quartz and montmorillonite, but this was far less significant than for goethite. These results suggest that H_2O_2 can promote the desorption of mineral-associated Pu(IV) in contaminated environments especially in the presence of Fe species. Given the ubiquity of Fe minerals such as goethite in the environment, this mechanism may be important in a number of scenarios including surface water environments experiencing rainfall input as well as seasonal changes in hydrogen peroxide-generating natural organic matter, subsurface environments where bacterial processes generate high levels of H_2O_2 , and nuclear waste repositories where H_2O_2 is formed by the effect of radiation on water. Further study is needed to elucidate the Pu desorption mechanism. There is also the potential that this desorption process will be relevant for other redox-active radionuclides, such as uranium or

neptunium, which show lower environmental mobility in the reduced oxidation state.

■ ASSOCIATED CONTENT

● Supporting Information

Additional information as noted in the text. This material is available free of charge via the Internet at <http://pubs.acs.org>.

■ AUTHOR INFORMATION

Corresponding Author

*E-mail: Begg2@llnl.gov.

Notes

This document was prepared as an account of work sponsored by an agency of the United States government. Neither the United States government nor Lawrence Livermore National Security, LLC, nor any of their employees makes any warranty, expressed or implied, or assumes any legal liability or responsibility for the accuracy, completeness, or usefulness of any information, apparatus, product, or process disclosed, or represents that its use would not infringe privately owned rights. Reference herein to any specific commercial product, process, or service by trade name, trademark, manufacturer, or otherwise does not necessarily constitute or imply its endorsement, recommendation, or favoring by the United States government or Lawrence Livermore National Security, LLC. The views and opinions of authors expressed herein do not necessarily state or reflect those of the United States government or Lawrence Livermore National Security, LLC, and shall not be used for advertising or product endorsement purposes.

The authors declare no competing financial interest.

■ ACKNOWLEDGMENTS

We thank Dr. R. Tinnacher (LBNL) for thought-provoking discussions and Dr. I. Cvijanovic (Carnegie Institution for Science, Stanford) for helpful suggestions. The flow cell was kindly provided by the B. Powell research group and manufactured at Clemson University. This work was supported by the Subsurface Biogeochemical Research Program of the U.S. Department of Energy's Office of Biological and Environmental Research. Prepared by LLNL under contract DE-AC52-07NA27344.

■ REFERENCES

- (1) Nelson, D. M.; Lovett, M. B. Oxidation state of plutonium in the Irish Sea. *Nature* **1978**, 276 (5688), 599–601.
- (2) Montero, P. R.; Sanchez, A. M. Plutonium contamination from accidental release or simply fallout: Study of soils at Palomares (Spain). *J. Environ. Radioact.* **2001**, 55 (2), 157–165.
- (3) Smith, D. K.; Finnegan, D. L.; Bowen, S. M. An inventory of long-lived radionuclides residual from underground nuclear testing at the Nevada test site, 1951–1992. *J. Environ. Radioact.* **2003**, 67 (1), 35–51.
- (4) Morris, K.; Butterworth, J. C.; Livens, F. R. Evidence for the remobilization of Sellafield waste radionuclides in an intertidal salt marsh, West Cumbria, UK. *Estuarine, Coastal Shelf Sci.* **2000**, 51 (5), 613–625.
- (5) Choppin, G. R. Redox speciation of plutonium in natural waters. *J. Radioanal. Nucl. Chem.-Art.* **1991**, 147 (1), 109–116.
- (6) Morgenstern, A.; Choppin, G. R. Kinetics of the reduction of Pu(V)O_2^+ by hydrogen peroxide. *Radiochim. Acta* **1999**, 86 (3–4), 109–113.
- (7) Kersting, A. B.; Efur, D. W.; Finnegan, D. L.; Rokop, D. J.; Smith, D. K.; Thompson, J. L. Migration of plutonium in ground water at the Nevada Test Site. *Nature* **1999**, 397 (6714), 56–59.
- (8) Novikov, A. P.; Kalmykov, S. N.; Utsunomiya, S.; Ewing, R. C.; Horreard, F.; Merkulov, A.; Clark, S. B.; Tkachev, V. V.; Myasoedov, B. F. Colloid transport of plutonium in the far-field of the Mayak Production Association, Russia. *Science* **2006**, 314 (5799), 638–641.
- (9) Santschi, P. H.; Roberts, K. A.; Guo, L. D. Organic nature of colloidal actinides transported in surface water environments. *Environ. Sci. Technol.* **2002**, 36 (17), 3711–3719.
- (10) Neck, V.; Altmaier, M.; Seibert, A.; Yun, J. I.; Marquardt, C. M.; Fanghanel, T. Solubility and redox reactions of Pu(IV) hydrous oxide: Evidence for the formation of $\text{PuO}_{2+x}(\text{s, hyd})$. *Radiochim. Acta* **2007**, 95 (4), 193–207.
- (11) Efur, D. W.; Runde, W.; Banar, J. C.; Janecky, D. R.; Kaszuba, J. P.; Palmer, P. D.; Roensch, F. R.; Tait, C. D. Neptunium and plutonium solubilities in a Yucca Mountain groundwater. *Environ. Sci. Technol.* **1998**, 32 (24), 3893–3900.
- (12) Begg, J. D.; Zavarin, M.; Zhao, P.; Tume, S. J.; Powell, B.; Kersting, A. B. Pu(V) and Pu(IV) sorption to montmorillonite. *Environ. Sci. Technol.* **2013**, 47 (10), 5146–5153.
- (13) Powell, B. A.; Fjeld, R. A.; Kaplan, D. I.; Coates, J. T.; Serkiz, S. M. Pu(V)O_2^+ adsorption and reduction by synthetic magnetite (Fe_3O_4). *Environ. Sci. Technol.* **2004**, 38 (22), 6016–6024.
- (14) Lu, N. P.; Reimus, P. W.; Parker, G. R.; Conca, J. L.; Triay, I. R. Sorption kinetics and impact of temperature, ionic strength and colloid concentration on the adsorption of plutonium-239 by inorganic colloids. *Radiochim. Acta* **2003**, 91 (12), 713–720.
- (15) Icopini, G. A.; Lack, J. G.; Hersman, L. E.; Neu, M. P.; Boukhalfa, H. Plutonium(V/VI) reduction by the metal-reducing Bacteria *Geobacter metallireducens* GS-15 and *Shewanella oneidensis* MR-1. *Appl. Environ. Microb.* **2009**, 75 (11), 3641–3647.
- (16) Zhao, P. H.; Zavarin, M.; Leif, R. N.; Powell, B. A.; Singleton, M. J.; Lindvall, R. E.; Kersting, A. B. Mobilization of actinides by dissolved organic compounds at the Nevada Test Site. *Appl. Geochem.* **2011**, 26 (3), 308–318.
- (17) Keeney-Kennicutt, W. L.; Morse, J. W. The redox chemistry of Pu(V)O_2^+ interaction with common mineral surfaces in dilute solutions and seawater. *Geochim. Cosmochim. Acta* **1985**, 49 (12), 2577–2588.
- (18) Sanchez, A. L.; Murray, J. W.; Sibley, T. H. The adsorption of plutonium IV and plutonium V on goethite. *Geochim. Cosmochim. Acta* **1985**, 49 (11), 2297–2307.
- (19) Silva, R. J.; Nitsche, H. Actinide environmental chemistry. *Radiochim. Acta* **1995**, 70–1, 377–396.
- (20) Choppin, G. R.; Bond, A. H.; Hromadka, P. M. Redox speciation of plutonium. *J. Radioanal. Nucl. Chem.* **1997**, 219 (2), 203–210.
- (21) Orlandini, K. A.; Penrose, W. R.; Nelson, D. M. Pu(V) as the stable form of oxidized plutonium in natural waters. *Mar. Chem.* **1986**, 18 (1), 49–57.
- (22) Powell, B. A.; Duff, M. C.; Kaplan, D. I.; Fjeld, R. A.; Newville, M.; Hunter, D. B.; Bertsch, P. M.; Coates, J. T.; Eng, P.; Rivers, M. L.; Sutton, S. R.; Triay, I. R.; Vanniman, D. T. Plutonium oxidation and subsequent reduction by Mn(IV) minerals in Yucca Mountain tuff. *Environ. Sci. Technol.* **2006**, 40 (11), 3508–3514.
- (23) Powell, B. A.; Fjeld, R. A.; Kaplan, D. I.; Coates, J. T.; Serkiz, S. M. Pu(V)O_2^+ adsorption and reduction by synthetic hematite and goethite. *Environ. Sci. Technol.* **2005**, 39 (7), 2107–2114.
- (24) Lujanienė, G.; Benes, P.; Stamberg, K.; Joksas, K.; Kulakauskaitė, I. Pu and Am sorption to the Baltic Sea bottom sediments. *J. Radioanal. Nucl. Chem.* **2013**, 295 (3), 1957–1967.
- (25) Buda, R. A.; Banik, N. L.; Kratz, J. V.; Trautmann, N. Studies of the ternary systems humic substances - kaolinite - Pu(III) and Pu(IV) . *Radiochim. Acta* **2008**, 96 (9–11), 657–665.
- (26) Zavarin, M.; Powell, B. A.; Bourbin, M.; Zhao, P. H.; Kersting, A. B. Np(V) and Pu(V) ion exchange and surface-mediated reduction mechanisms on montmorillonite. *Environ. Sci. Technol.* **2012**, 46 (5), 2692–2698.

- (27) Hixon, A. E.; Arai, Y.; Powell, B. A. Examination of the effect of alpha radiolysis on plutonium(V) sorption to quartz using multiple plutonium isotopes. *J. Colloid Interface Sci.* **2013**, *403* (0), 105–112.
- (28) Kaplan, D. I.; Powell, B. A.; Duff, M. C.; Demirkanli, D. I.; Denham, M.; Fjeld, R. A.; Molz, F. J. Influence of sources on plutonium mobility and oxidation state transformations in vadose zone sediments. *Environ. Sci. Technol.* **2007**, *41* (21), 7417–7423.
- (29) Romanchuk, A. Y.; Kalmykov, S. N.; Aliev, R. A. Plutonium sorption onto hematite colloids at femto- and nanomolar concentrations. *Radiochim. Acta* **2011**, *99* (3), 137–144.
- (30) Felmy, A. R.; Moore, D. A.; Rosso, K. M.; Qafoku, O.; Rai, D.; Buck, E. C.; Ilton, E. S. Heterogeneous reduction of PuO_2 with Fe(II) : Importance of the Fe(III) reaction product. *Environ. Sci. Technol.* **2011**, *45* (9), 3952–3958.
- (31) Kirsch, R.; Fellhauer, D.; Altmaier, M.; Neck, V.; Rossberg, A.; Fanghanel, T.; Charlet, L.; Scheinost, A. C. Oxidation state and local structure of plutonium reacted with magnetite, mackinawite, and chukanovite. *Environ. Sci. Technol.* **2011**, *45* (17), 7267–7274.
- (32) Lu, N.; Cotter, C. R.; Kitten, H. D.; Bentley, J.; Triay, I. R. Reversibility of sorption of plutonium-239 onto hematite and goethite colloids. *Radiochim. Acta* **1998**, *83* (4), 167–173.
- (33) Hamilton-Taylor, J.; Kelly, M.; Mudge, S.; Bradshaw, K. Rapid remobilization of plutonium from estuarine sediments. *J. Environ. Radioact.* **1987**, *5* (6), 409–423.
- (34) Kaplan, D. I.; Powell, B. A.; Gumapas, L.; Coates, J. T.; Field, R. A.; Diprete, D. P. Influence of pH on plutonium desorption/solubilization from sediment. *Environ. Sci. Technol.* **2006**, *40*, 5937–5942.
- (35) McCubbin, D.; Leonard, K. S. Photochemical dissolution of radionuclides from marine sediments. *Mar. Chem.* **1996**, *55*, 399–408.
- (36) Burke, I. T.; Boothman, C.; Lloyd, J. R.; Livens, F. R.; Charnock, J. M.; McBeth, J. M.; Mortimer, R. J. G.; Morris, K. Reoxidation behavior of technetium, iron, and sulfur in estuarine sediments. *Environ. Sci. Technol.* **2006**, *40* (11), 3529–3535.
- (37) Law, G. T. W.; Geissler, A.; Lloyd, J. R.; Livens, F. R.; Boothman, C.; Begg, J. D. C.; Denecke, M. A.; Rothe, J.; Dardenne, K.; Burke, I. T.; Charnock, J. M.; Morris, K. Geomicrobiological redox cycling of the transuranic element neptunium. *Environ. Sci. Technol.* **2010**, *44* (23), 8924–8929.
- (38) Moon, H. S.; Komlos, J.; Jaffe, P. R. Uranium reoxidation in previously bioreduced sediment by dissolved oxygen and nitrate. *Environ. Sci. Technol.* **2007**, *41* (13), 4587–4592.
- (39) Begg, J. D. C.; Burke, I. T.; Charnock, J. M.; Morris, K. Technetium reduction and reoxidation behaviour in Dounreay soils. *Radiochim. Acta* **2008**, *96* (9–11), 631–636.
- (40) Sani, R. K.; Peyton, B. M.; Dohnalkova, A.; Amonette, J. E. Reoxidation of reduced uranium with iron(III) (hydr)oxides under sulfate-reducing conditions. *Environ. Sci. Technol.* **2005**, *39* (7), 2059–2066.
- (41) Balakrishnan, P. V.; Mazumdar, A. S. G. Observations on the action of hydrogen peroxide on trivalent and tetravalent plutonium solutions. *J. Inorg. Nucl. Chem.* **1964**, *26* (5), 759–765.
- (42) Clark, D.; Hecker, S.; Jarvinen, G.; Neu, M. Plutonium. In *The Chemistry of the Actinide and Transactinide Elements*; Morss, L.; Edelstein, N.; Fuger, J., Eds.; Springer: Dordrecht, Netherlands, 2011; pp 813–1264.
- (43) Hagan, P. G.; Miner, F. J. Plutonium peroxide precipitation: Review and current research. In *Actinide Separations*; American Chemical Society: Washington, DC, 1980; Vol. 117, pp 51–67.
- (44) Shilov, V. P.; Astafurova, L. N.; Garnov, A. Y.; Krot, N. N. Reaction of H_2O_2 with suspensions of Np(OH)_4 and Pu(OH)_4 in alkali solution. *Radiochemistry* **1996**, *38* (3), 217–219.
- (45) Sill, C. W.; Percival, D. R.; Williams, R. L. Catalytic effect of iron on oxidation of plutonium by hydrogen peroxide. *Anal. Chem.* **1970**, *42* (11), 1273–8.
- (46) Cooper, W. J.; Lean, D. R. S. Hydrogen peroxide concentration in a northern lake: Photochemical formation and diel variability. *Environ. Sci. Technol.* **1989**, *23* (11), 1425–1428.
- (47) Zika, R. G.; Moffett, J. W.; Petasne, R. G.; Cooper, W. J.; Saltzman, E. S. Spatial and temporal variations of hydrogen-peroxide in Gulf of Mexico waters. *Geochim. Cosmochim. Acta* **1985**, *49* (5), 1173–1184.
- (48) Gonzalez-Flecha, B.; Demple, B. Homeostatic regulation of intracellular hydrogen peroxide concentration in aerobically growing *Escherichia coli*. *J. Bacteriol.* **1997**, *179* (2), 382–388.
- (49) Guillen, F.; Martinez, A. T.; Martinez, M. J. Production of hydrogen-peroxide by aryl-alcohol oxidase from the ligninolytic fungus *Pleurotus eryngii*. *Appl. Microbiol. Biotechnol.* **1990**, *32* (4), 465–469.
- (50) Kok, G. L. Measurements of hydrogen-peroxide in rainwater. *Atmos. Environ.* **1980**, *14* (6), 653–656.
- (51) Watts, R. J.; Finn, D. D.; Cutler, L. M.; Schmidt, J. T.; Teel, A. L. Enhanced stability of hydrogen peroxide in the presence of subsurface solids. *J. Contam. Hydrol.* **2007**, *91* (3–4), 312–326.
- (52) Li, H. P.; Yeager, C. M.; Brinkmeyer, R.; Zhang, S. J.; Ho, Y. F.; Xu, C.; Jones, W. L.; Schwehr, K. A.; Otosaka, S.; Roberts, K. A.; Kaplan, D. I.; Santschi, P. H. Bacterial production of organic acids enhances H_2O_2 -dependent iodide oxidation. *Environ. Sci. Technol.* **2012**, *46* (9), 4837–4844.
- (53) Christensen, H. Calculations simulating spent-fuel leaching experiments. *Nucl. Technol.* **1998**, *124* (2), 165–174.
- (54) Amme, M.; Bors, W.; Michel, C.; Stettmaier, K.; Rasmussen, G.; Betti, M. Effects of Fe(II) and hydrogen peroxide interaction upon dissolving UO_2 under geologic repository conditions. *Environ. Sci. Technol.* **2005**, *39* (1), 221–229.
- (55) Amme, M.; Pehrman, R.; Deutsch, R.; Roth, O.; Jonsson, M. Combined effects of Fe(II) and oxidizing radiolysis products on UO_2 and PuO_2 dissolution in a system containing solid UO_2 and PuO_2 . *J. Nucl. Mater.* **2012**, *430* (1–3), 1–5.
- (56) Voelker, B. M.; Sulzberger, B. Effects of fulvic acid on Fe(II) oxidation by hydrogen peroxide. *Environ. Sci. Technol.* **1996**, *30* (4), 1106–1114.
- (57) Kwan, W. P.; Voelker, B. M. Decomposition of hydrogen peroxide and organic compounds in the presence of dissolved iron and ferrihydrite. *Environ. Sci. Technol.* **2002**, *36* (7), 1467–1476.
- (58) Hug, S. J.; Leupin, O. Iron-catalyzed oxidation of arsenic(III) by oxygen and by hydrogen peroxide: pH-dependent formation of oxidants in the Fenton reaction. *Environ. Sci. Technol.* **2003**, *37* (12), 2734–2742.
- (59) Voegelin, A.; Hug, S. J. Catalyzed oxidation of arsenic(III) by hydrogen peroxide on the surface of ferrihydrite: An in situ ATR-FTIR study. *Environ. Sci. Technol.* **2003**, *37* (5), 972–978.
- (60) Pettine, M.; Millero, F. J. Effect of metals on the oxidation of As(III) with H_2O_2 . *Mar. Chem.* **2000**, *70* (1–3), 223–234.
- (61) Powell, B. A.; Dai, Z. R.; Zavarin, M.; Zhao, P. H.; Kersting, A. B. Stabilization of plutonium nano-colloids by epitaxial distortion on mineral surfaces. *Environ. Sci. Technol.* **2011**, *45* (7), 2698–2703.
- (62) Kobashi, A.; Choppin, G. R. A study of techniques for separating plutonium in different oxidation states. *Radiochim. Acta* **1988**, *43*, 211–215.
- (63) Tinnacher, R. M.; Zavarin, M.; Powell, B. A.; Kersting, A. B. Kinetics of neptunium(V) sorption and desorption on goethite: An experimental and modeling study. *Geochim. Cosmochim. Acta* **2011**, *75* (21), 6584–6599.
- (64) Lovley, D. R.; Phillips, E. J. P. Availability of ferric iron for microbial reduction in bottom sediments of the freshwater tidal Potomac River. *Appl. Environ. Microb.* **1986**, *52* (4), 751–757.
- (65) Unimin Iota High Purity Quarz Technical Data. <http://www.iotaquartz.com/pdfs/Iota-Semi-VIF.pdf>.
- (66) Noble, R. W.; Gibson, Q. H. Reaction of ferrous horseradish peroxidase with hydrogen peroxide. *J. Biol. Chem.* **1970**, *245* (9), 2409–2413.
- (67) Viollier, E.; Inglett, P. W.; Hunter, K.; Roychoudhury, A. N.; Van Cappellen, P. The ferrozine method revisited: Fe(II)/Fe(III) determination in natural waters. *Appl. Geochem.* **2000**, *15* (6), 785–790.
- (68) Zhou, M. J.; Diwu, Z. J.; PanchukVoloshina, N.; Haugland, R. P. A stable nonfluorescent derivative of resorufin for the fluorometric

determination of trace hydrogen peroxide: Applications in detecting the activity of phagocyte NADPH oxidase and other oxidases. *Anal. Biochem.* **1997**, 253 (2), 162–168.

(69) Invitrogen Amplex Red Hydrogen Peroxide/Peroxidase Assay Kit. <http://tools.lifetechnologies.com/content/sfs/manuals/mp22188.pdf>.

(70) Pham, A. L. T.; Doyle, F. M.; Sedlak, D. L. Inhibitory effect of dissolved silica on H_2O_2 decomposition by iron(III) and manganese(IV) oxides: Implications for H_2O_2 -based in situ chemical oxidation. *Environ. Sci. Technol.* **2012**, 46 (2), 1055–1062.

(71) Lin, S. S.; Gurol, M. D. Catalytic decomposition of hydrogen peroxide on iron oxide: Kinetics, mechanism, and implications. *Environ. Sci. Technol.* **1998**, 32 (10), 1417–1423.